

Creep, creep recovery and dynamic mechanical measurements of a poly(propylene glycol) oligomer

J. Cochrane, G. Harrison, J. Lamb and D. W. Phillips*

Department of Electronics and Electrical Engineering, The University, Glasgow G12 8QQ, UK

(Received 24 September 1979)

Measurements have been made of the viscoelastic properties of a low molecular mass poly(propylene glycol), P4000, in shear creep and creep recovery. Taken together with previous dynamic mechanical measurements in alternating shear at frequencies of 30 MHz and 454 MHz and additional dynamic measurements at 40 kHz, it is shown that the observed behaviour can be ascribed to two processes. The major contribution can be associated with the normal modes of the polymer molecule as a whole but a significant contribution is attributed to motions of smaller backbone units, akin to the behaviour of supercooled non-polymeric liquids. The latter are described by a complex compliance which must first be inverted to the modulus form before addition to the summation of Rouse modes in order to calculate the effective overall modulus. Retardation times associated with motions of the backbone units overlap the relaxation times of the higher order Rouse modes which are apparently rendered inactive, the polymer mode contribution being accounted for by either the first or, at most, the first two Rouse modes. The equilibrium compliance, J_e^0 , decreases markedly with decreasing temperature within 15K above the glass transition temperature. At higher temperatures ($> T_g + 15$ K) J_e^0 decreases gradually with increasing temperature in agreement with calculations based upon the combined polymer mode and backbone processes. Particular care was necessary in order to obtain thoroughly dry samples of P4000: the presence of relatively small amounts of water increased the value of J_e^0 by up to four orders of magnitude.

INTRODUCTION

Previous publications from this laboratory have reported measurements of the dielectric and high-frequency dynamic mechanical response of low molecular mass poly(propylene glycols)^{1,2}. The oligomer of nominal molecular mass 400 (P400) showed one dispersion region which could be described by the Williams–Watts function with $\beta = 0.51$ for dielectric relaxation and by the Davidson–Cole function with $\beta = 0.45$ for mechanical retardation. Although the time constants sensed by the different techniques were up to a decade apart, there could be little doubt that the same fundamental molecular motion was involved. Such processes appear to be characteristic of low molecular mass glass-forming liquids and have been ascribed to local segmental motion³.

The higher molecular mass poly(glycol), P4000, responded in a different manner. Dielectrically, this polymer gave rise to a dispersion with a very similar time constant and relative breadth to that of the P400. However, there was, in addition, a smaller, molecular mass dependent, dispersion region having a characteristic relaxation time some three orders of magnitude greater than that of the dominant process. This longer-time process was not clearly resolved in the dynamic mechanical experiment but has been ascribed dielectrically to co-operative dipole relaxations, which involve only the even numbered modes³, although the narrowness of the dis-

person would seem to contradict this. The viscoelastic properties of the P4000 were shown to differ from those of the P400 by an additional retardation or relaxation process for the higher molecular mass material. This can be attributed to the appearance of some polymeric or normal mode behaviour in the P4000.

An attempt has therefore been made to reconcile the dielectric and mechanical results with normal mode theory by measuring the viscoelastic response of P4000 in shear creep. In particular, since creep experiments involve much longer time scales than are readily accessible with dynamic experiments, it was thought that it would thereby be possible to examine the low frequency response in more detail.

The dynamic compliance of linear viscoelastic materials may be described by the complex compliance, J^* , where:

$$J^*(j\omega) = J'(\omega) - jJ''(\omega) \quad (1)$$

$$= J_\infty + \frac{1}{j\omega\eta} + J_r\chi(j\omega) \quad (2)$$

The frequency dependence of the retardational compliance is described by $\chi(j\omega)$, J_∞ is the infinite frequency or glassy compliance and η is the limiting low frequency or steady flow viscosity. Alternatively, the behaviour may be described in terms of a complex modulus:

$$G^*(j\omega) = 1/J^*(j\omega) = G'(\omega) + jG''(\omega) \quad (3)$$

* Present address: S. R. D., Culcheth, Warrington, UK

Table 1 Molecular mass data for poly(propylene glycol) oligomers*

Nominal	\bar{M}_n (osmometry)	\bar{M}_n	\bar{M}	\bar{M}_z	\bar{M}_{z+1}
400	380	320	330	340	350
1200	630	670	720	770	810
2000	1560	1460	1600	1860	2060
4000	3030	4020	4350	8640	49 500

* Provided by the G.P.C. Service, Department of Pure and Applied Chemistry, University of Strathclyde

The steady shear experiment gives the creep compliance, $J(t)$, defined by:

$$J(t) = J_\infty + t/\eta + J_r \psi(t) \quad (4)$$

In practice, the torque is removed after steady shear flow conditions have been attained. Measurements are then made of the subsequent creep recovery, giving:

$$J_d(t) = J(t) - t/\eta = J_\infty + J_r \psi(t)$$

$J(t)$ and $J^*(j\omega)$ are related by their Fourier transforms. The retardation functions χ and ψ are more simply related through the normalized spectrum of retardation times, $N(\tau)$:

$$\chi(j\omega) = \int_0^\infty \frac{N(\tau) d\tau}{1 + j\omega\tau} \quad (5)$$

$$\psi(t) = \int_0^\infty N(\tau) [1 - e^{-t/\tau}] d\tau \quad (6)$$

EXPERIMENTAL

Details of the molecular masses of the poly(propylene glycol) melts are given in Table 1. All the samples have fairly narrow molecular mass distributions ($\bar{M}/\bar{M}_n < 1.16$, where \bar{M} denotes the mass average) and are stereo-irregular. There is, however, evidence of a distinct high molecular mass tail, particularly in the P4000. Before any measurements were made, the samples were carefully dried and outgassed by baking *in vacuo* at 100°C for 30 hours according to standard procedure. In the light of subsequent information on residual water content, dry samples were prepared by further treatment at 120°C *in vacuo* for 120 hours. This procedure had no measurable effect upon the steady flow viscosity, this being taken as evidence for the absence of degradation.

Viscosities of the P400 and P4000 have been reported previously¹: those of the P1200 and P2000 were likewise determined with suspended level viscometers over the temperature range -20°C to +70°C. All these results, covering viscosities up to 50 Pa s, fit the modified free volume equation:

$$\ln(\eta) = A + B/(T - T_0) \quad (7)$$

Density values for each oligomer showed a simple temperature dependence:

$$\rho = \rho_0 [1 - \gamma(T - T_0)] \quad (8)$$

Values of the parameters of equations (7) and (8) are given in Table 2.

The components R_L and X_L of the mechanical shear impedance of P4000 were measured using travelling torsional waves at 40.0 kHz over the temperature range -30°C to 0°C: the estimated error in both components is $\pm 5\%$ ⁴. From these data the complex shear compliance and its components may be calculated:

$$J'(\omega) = \rho(R_L^2 - X_L^2)/(R_L^2 + X_L^2)^2 \quad (9)$$

$$J''(\omega) = 2\rho R_L X_L/(R_L^2 + X_L^2)^2 \quad (10)$$

These results cover the temperature-frequency region between the previously published 30 MHz and 454 MHz results and the present shear creep and creep recovery measurements.

The viscosity and creep recovery of P4000 were measured over the temperature range -76°C to +10°C. The magnetic bearing creep machine used was similar to that described by Plazek⁵. The instrument was capable of measuring viscosities from 10⁻¹ Pa s to 10¹⁴ Pa s to better than $\pm 5\%$ and recoverable compliances from 10⁻¹⁰ Pa⁻¹ to 10⁻¹ Pa⁻¹ to better than $\pm 8\%$. The sample temperature was controlled to within ± 0.1 K over the entire range of temperature using a well-stirred alcohol bath. Experimental runs were made from times of 0.1 s to 10⁵ s, giving six decades of direct measurement. All the creep measurements were made under an atmosphere of dry nitrogen or dry helium, special care being taken to avoid any sample contamination.

RESULTS AND ANALYSIS

Initial creep recovery measurements of P4000 indicated exceptionally high values for the limiting long-time (steady state) recoverable compliance, $J_e^0 (= J_r + J_\infty)$, in the region of 10⁻³ Pa⁻¹. It was also noted that these values of J_e^0 showed a strong dependence upon shear rate. These values are substantially greater than the values observed for other low molecular mass polymers, which are typically in the region of 10⁻⁶ Pa⁻¹⁶.

Previous publications have referred to the ability of low molecular mass poly(ethylene oxide) to form relatively stable complexes with water⁷. Similar hydration processes might be expected with poly(propylene glycol) in view of the hygroscopic nature of this polymer. Therefore, the P4000 was re-baked *in vacuo* at 120°C for 120 hours and re-measured. The viscosity was sensibly unaltered, while J_e^0 was now found to be within the expected range of values. Also, J_e^0 for the dried sample was independent of the stress level over the range of stresses available.

Figure 1 shows the creep recovery of the dried sample as a function of time at various temperatures. Empirical

Table 2 Viscosity and density parameters of equations (7) and (8)

Oligomer	A	B/K	T ₀ /K	ρ ₀ /kgm ⁻³	10 ⁴ γ/K ⁻¹
P400	-10.774	1047.3	168.4	1116	7.27
P1200	-8.756	828.7	180.3	1092	6.98
P2000	-8.134	846.6	178.1	1093	7.07
P4000	-7.172	817.2	180.1	1063	6.96

All viscosity values in Pa s. (capillary viscometer measurements)

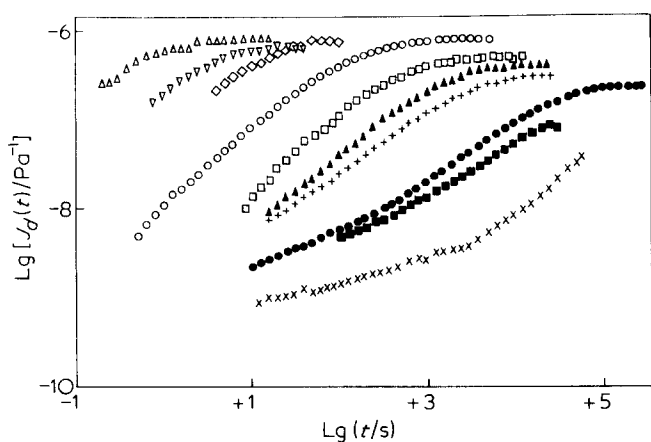


Figure 1 Recoverable compliance, $J_d(t)$, of dry P4000 plotted against time at the following temperatures: \triangle , -50.5°C ; ∇ , -62.4°C ; \diamond , -64.6°C ; \circ , -68.0°C ; \square , -69.6°C ; \blacktriangle , -70.9°C ; $+$, -72.3°C ; \bullet , -74.0°C ; \blacksquare , -75.0°C ; \times , -76.0°C

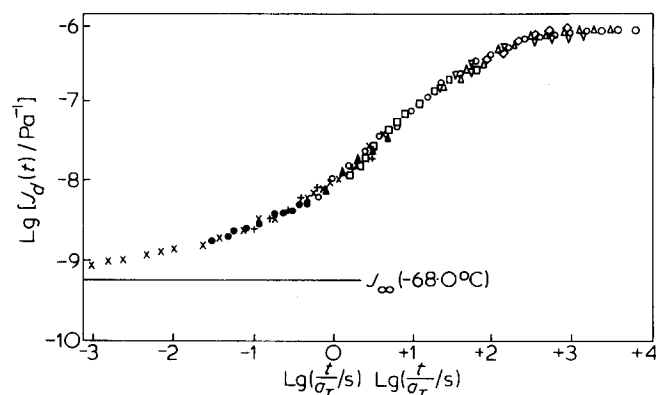


Figure 2 Recoverable compliance, $J_d(t)$, of dry P4000 plotted against time and reduced to -68.0°C by the use of empirical horizontal shift factors. Key as Figure 1. J_∞ values at -68.0°C taken from dynamic measurements of Barlow and Erginsav¹

superposition of these individual recovery curves for temperatures above -68°C gave a master recovery curve at -68°C , Figure 2. This superposition was achieved using only shifts along the time axis; shifts along the compliance axis were not found necessary since neither the J_e^0 nor the J_∞ values exhibited any significant temperature dependence over the range of measurement. It is, however, apparent from Figure 1 that at temperatures below -68°C , J_e^0 shows a strong temperature dependence. For this temperature range, only the shorter time values of recoverable compliance, corresponding to values of $J_d(t) < 2 \times 10^{-8} \text{ Pa}^{-1}$, were incorporated into the master curve.

The time shift factors, a_T , necessary for the superposition of the creep recovery curves are shown in Figure 3. The temperature dependence of $\alpha = (\tau_m)_T / (\tau_m)_{-68^\circ\text{C}}$ where $\tau_m = \eta J_\infty$, is also shown in Figure 3. With the exception of the value at -50.5°C , both α and a_T have a very similar temperature dependence. The value at -50.5°C corresponded to the shortest measurement time and the smallest angular deflection and was consequently subject to a significantly greater error. Values of a_T from 40°C to 80°C are obtained from dynamic measurements at 30 MHz¹, and from -30°C to 0°C using the 40 kHz measurements as described in the section headed 'Interpretation and Discussion'.

The viscosity values obtained from creep (3.5 Pa s to $4.4 \times 10^{11} \text{ Pa s}$) and capillary viscometer measurements were

together fitted by a modified free volume equation of the form given in equation (7):

$$\ln(\eta/\text{Pa s}) = -7.94 + 1018.4 (T/\text{K} - 166.7) \quad (11)$$

The standard deviation from this line was $\pm 1.2\%$ over the entire range of temperatures from -76°C to $+80^\circ\text{C}$. In the limited range of temperatures where both creep and capillary viscometer viscosity values could be obtained, the calculated and measured values agreed with experimental error, although the differences in the A , B , T_0 values (equation (11) and Table 2) are considerable. This illustrates the errors which can result from the extrapolation of A , B , T_0 equations well beyond the range of measurement.

The temperature dependence of J_e^0 for P4000 is shown in Figure 4 with, for comparison, the same parameter for two narrow distribution poly(styrenes) of molecular masses 3500 and 10 200. The latter measurements have been published and discussed elsewhere⁶. All the measurements are normalized with respect to the glass transition temperature, T_g , at which temperature the viscosity is $1 \times 10^{12} \text{ Pa s}$. The marked decrease in J_e^0 at temperatures near T_g which occurs in these three polymers has also been found in other narrow distribu-

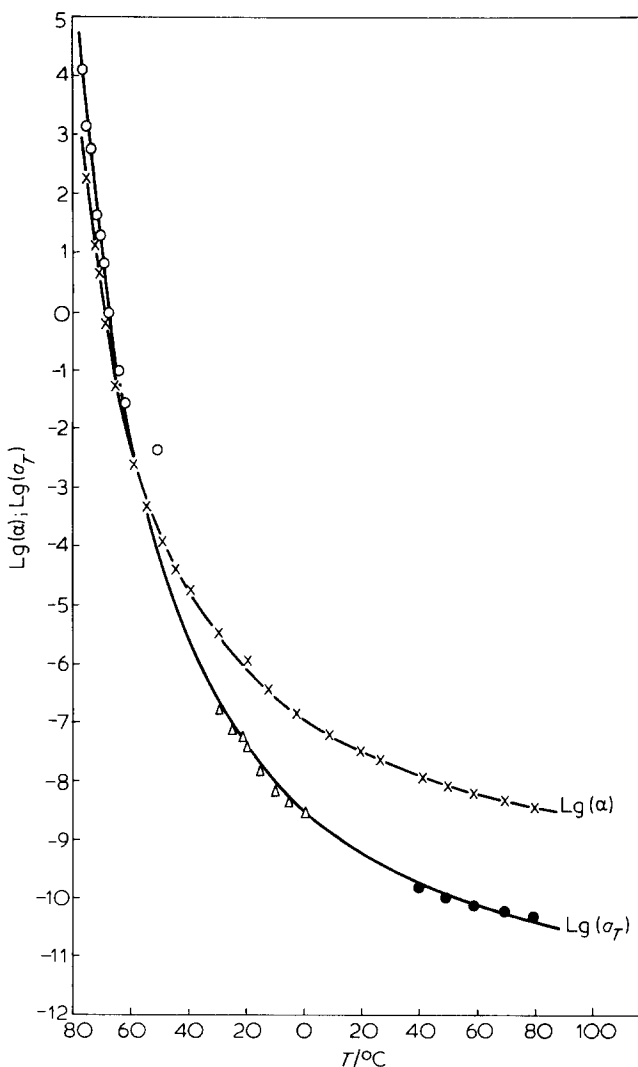


Figure 3 Temperature variation of $\alpha = (\tau_m)_T / (\tau_m)_{-68}$, \times , and the empirical time scale shift factor, a_T , obtained from measurements of creep recovery, \circ , and dynamic measurements at 40 kHz, \triangle , and 30 MHz, \bullet

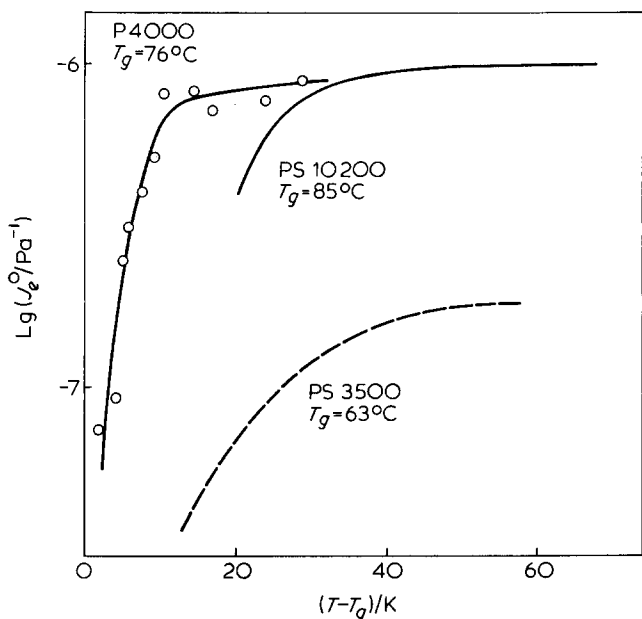


Figure 4 Equilibrium recoverable compliance, J_e^0 , of P4000 (○), PS3500 (---) and PS10200 (—) plotted as a function of reduced temperature. Poly(styrene) data taken from Gray *et al.*⁶

tion poly(styrenes)⁸. These authors reported a reduction with increasing molecular mass of the temperature interval over which J_e^0 changed markedly. It appears from Figure 4 that this temperature interval depends also upon polymer structure, the more flexible backbone of the poly(propylene glycol) being associated with a smaller interval.

The value of J_e^0 for the 10 200 poly(styrene) was found to agree well with the value expected from Rouse theory for a monodisperse low molecular mass polymer melt⁹:

$$J_e^0 = 0.4 M/\rho RT \quad (12)$$

The molecular mass data given in Table 1 show the presence of a high molecular mass tail in the P4000. This tail is partly responsible for the similarity in J_e^0 values for the P4000 and 10 200 poly(styrene). However, other effects influence the value of J_e^0 and these will be discussed in the section headed 'Interpretation and Discussion'.

Figure 5 shows creep recovery measurements at various temperatures and shear rates for the material as originally treated to remove water, together with the creep recovery at -68°C for the fully dried material, all reduced to a temperature of -68°C . Increasing shear rate produced a proportionate decrease in the equilibrium recoverable compliance. This increase in J_e^0 of up to four decades above the value for the dried sample was not accompanied by any measurable change in the steady state viscosity. To establish that water was responsible for the increase in J_e^0 the re-dried P4000 was mixed with 1% w/v of deionised, filtered water. The solution viscosity was only 5% less than the melt viscosity, while J_e^0 was again found to be non-linear with stress and had increased to a value of about 10^{-4} Pa^{-1} , Figure 5.

The details of this phenomenon remain speculative in the absence of other, structure sensitive, spectroscopic or scattering data. The effects on $J_r(t)$ resembled those caused by high molecular weight 'tails' in otherwise narrow distribution poly(styrenes)¹⁰. A small proportion of high molecular mass material can have a significant influence upon long time recoveries. This is because J_e^0 is related to the first moment of the relaxation spectrum, $H(\tau)$:

$$J_e^0 = (1/\eta^2) \int_{-\infty}^{\infty} \tau^2 H(\tau) d(\ln \tau) \quad (13)$$

whereas η is related to the zeroth moment:

$$\eta = \int_{-\infty}^{\infty} \tau H(\tau) d(\ln \tau) \quad (14)$$

Thus, J_e^0 is more sensitive to the long time properties of $H(\tau)$ and can be influenced by mechanisms too weak to produce measurable differences in η . It seemed likely that such properties could be associated with P4000 molecules linked extensively by hydrogen bonded water. The J_e^0 and τ values of the 'wet' P4000 corresponded to molecular masses of about 10^6 or aggregations of about 300 molecules. A weight fraction of 0.6% water would be adequate to achieve 100% conversion to linear combinations of this size, assuming that bonding occurred *via* hydrogen bonds at the chain terminating hydroxyl groups. Such large and relatively weakly-bonded networks would probably break up in high stress fields and give rise to the observed non-linearity in J_e^0 as a function of applied shear stress.

In order to interpret the creep recovery measurements in terms of previously established models⁶, interpolated values taken from the master creep curve of Figure 2 were transformed to the frequency domain, using an approximation developed by Schwarzl and Struik¹¹:

$$J'(t^{-1}) \cong 1.47 J(1.06t) - 0.87 J(4.37t) + 0.39 J(5.76t) \quad (15)$$

$$J''(t^{-1}) \cong 0.47 [J(4t) - J(2t)] + 1.72 [J(2t) - J(t)] + 0.90 [J(t/2) - J(t/4)] \quad (16)$$

(where $t^{-1} \equiv \omega$ and $\tan \delta(\omega) > 0.75$).

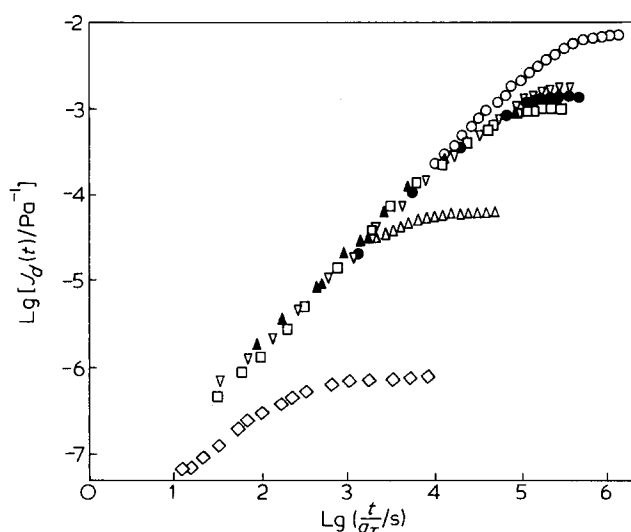


Figure 5 Recoverable compliance, $J_d(t)$, of water contaminated P4000 as a function of temperature and shear rate. ○, -25.3°C , $\dot{\gamma} = 0.33 \text{ s}^{-1}$; ▽, -50.1°C , $\dot{\gamma} = 0.16 \text{ s}^{-1}$; ●, -34.4°C , $\dot{\gamma} = 0.025 \text{ s}^{-1}$; □, -48.1°C , $\dot{\gamma} = 0.020 \text{ s}^{-1}$; ▲, -40.2°C , $\dot{\gamma} = 0.019 \text{ s}^{-1}$, dried P4000 (◇, -68.0°C) and a 99% w/v aqueous solution (△, -41.8°C). All data reduced to -68.0°C

Values of $J'(\omega)$ and $J''(\omega)$ were calculated at half-decade intervals using equations (15) and (16). Regions of sharper curvature were investigated in greater detail, using values of $J'(\omega)$ and $J''(\omega)$ calculated at fifth-decade intervals. The components of the complex modulus, $G'(\omega)$ and $G''(\omega)$, were calculated from the components of the complex compliance using equation (3). The resulting curves are shown as dashed lines in Figure 6. Similar curves resulted from using a transform approximation due to Yagii and Maekawa¹².

Previous viscoelastic measurements have shown that it is possible to describe the frequency dependence of the dynamic modulus using a model which combines two contributions⁶. These two contributions, at low and high frequencies, are formalized in terms of a limited number of Rouse modes and a distributed Davidson–Cole process, respectively:

$$G^*(j\omega) = G^*(j\omega)_{\text{Rouse}} + 1/J^*(j\omega)_{\text{DC}} \quad (17)$$

where:

$$G^*(j\omega)_{\text{Rouse}} = \frac{\rho RT}{M} \sum_{i=1}^n j\omega\tau_i / (1 + j\omega\tau_i) \quad (18)$$

$$\tau_i = \eta_R M / (i^2 \rho RT) \sum_{i=1}^n 1/i^2 \quad (19)$$

and:

$$J^*(j\omega)_{\text{DC}} = J_\infty + 1/j\omega\eta_{\text{DC}} + J_{r\text{DC}} / (1 + j\omega\tau_r)^\beta \quad (20)$$

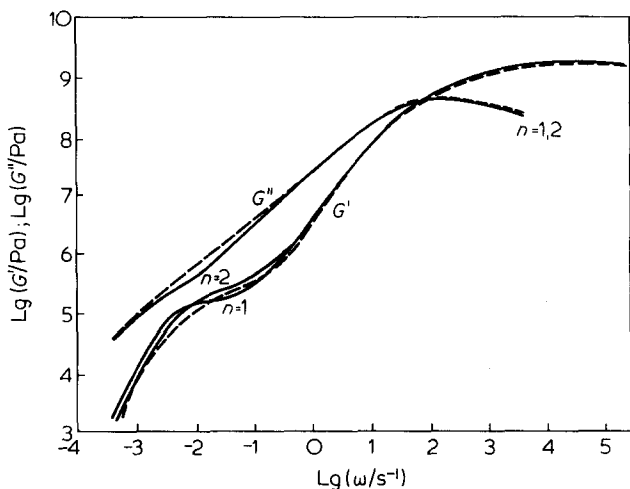


Figure 6 Frequency dependence of $G'(\omega)$ and $G''(\omega)$ for P4000 calculated from the transformed values of $J_G(t)$ shown in Figure 2 (---), together with the curves calculated from the combined Rouse and Davidson-Cole model (—) showing the effects of a variation in the number of active Rouse modes

Values of the model parameters which gave the best fit to the transformed measurements were:

(1) for the Davidson–Cole process

$$J_\infty = 5.63 \times 10^{-10} \text{ Pa}^{-1}, \eta_{\text{DC}} = (\eta)_{-68^\circ\text{C}} - \eta_R \\ = 3.44 \times 10^7 \text{ Pa s}$$

$$J_{e\text{DC}} = J_\infty + J_{r\text{DC}} = 1 \times 10^{-7} \text{ Pa}^{-1}$$

$$\tau_r = 10^4 \eta_{\text{DC}} J_\infty \quad \beta = 0.50$$

(2) for the Rouse process

$$M = 9500, T = -68^\circ\text{C}, \eta_R = 5.33 \times 10^7 \text{ Pa s}, n = 1 \text{ or } 2$$

The curves calculated using the above values of the parameters in equations (17) to (20) are compared in Figure 6 with the curves for G' and G'' derived from the transformed creep recovery measurements of Figure 2. Curves for higher values of mode number are not plotted, since they show an increasing departure from the experimentally derived curves, particularly in the case of G' .

The additional dynamic measurements were made in this laboratory at a frequency of 40 kHz by Dr R. W. Gray over the temperature range 0°C – 30°C and the results are given in Table 3.

INTERPRETATION AND DISCUSSION

The most significant feature of the experimental curves shown in Figure 6 is the pronounced shoulder in G' occurring at a frequency of about $10^{-1} \text{ rad s}^{-1}$. This feature was not observed in previous measurements made on low molecular mass poly(styrenes)⁶. It was found possible to describe the viscoelastic behaviour of the poly(styrenes) using either an overall Davidson–Cole model or a combined Davidson–Cole and Rouse model. The presence of the G' shoulder in the P4000 measurements did not, however, allow an adequate description of these measurements using the Davidson–Cole model alone.

Of the eight disposable parameters in the combined model, J_∞ and $\eta = \eta_R + \eta_{\text{DC}}$ can be determined by direct measurement. The temperature variation of J_∞ has been reported previously¹ as:

$$J_\infty / \text{Pa}^{-1} = 3.82 \times 10^{-10} + 1.85 \times 10^{-11} (T - T_g) / \text{K} \quad (21)$$

where T_g is taken as 195.3K.

The parameters τ_r and β of the Davidson–Cole model affect primarily the shape and position of the high frequency region ($\omega > 10 \text{ rad s}^{-1}$). The value of the distribution parameter, β , chosen to give the best fit in this frequency region, is 0.50. This is close to the value of 0.45 previously reported as giving the best fit to dynamic measurements made on a low molecular mass poly(propylene glycol), P400¹. As with

Table 3 Values of $J'(\omega)$ and $J''(\omega)$ calculated from 40 kHz dynamic measurements on P4000

$T/^\circ\text{C}$	+0.3	−5.2	−10.2	−15.8	−20.2	−22.2	−22.4	−25.0	−29.3
J'/GPa^{-1}	482	416	358	242	146	99	111	64	31
J''/GPa^{-1}	809	616	501	332	223	172	183	133	79

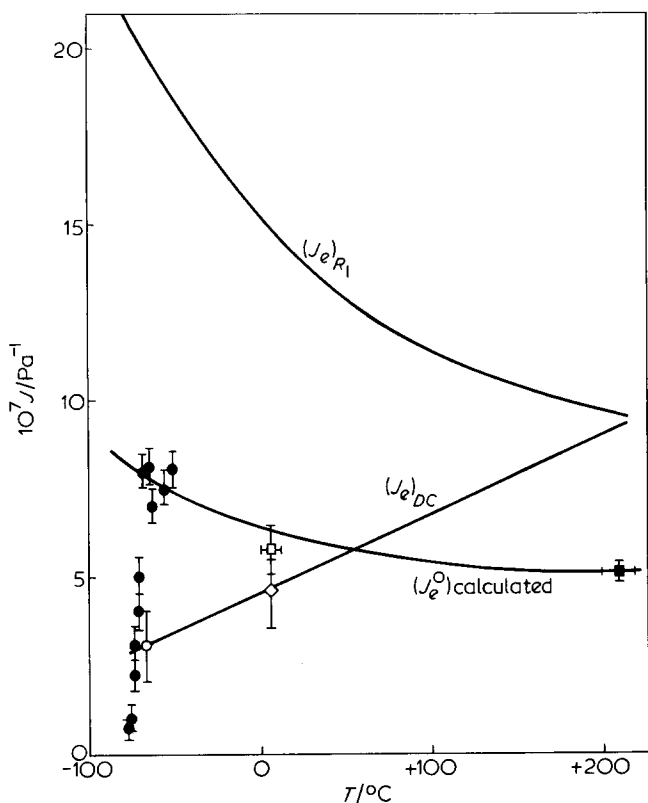


Figure 7 Temperature dependence of J_e^0 , J_{eR} and J_{eDC} for P4000. J_{eR} calculated from equation (12) using $M = 9500$. J_{eDC} values from creep (\circ) and 40 kHz (\diamond) measurements; the extrapolated J_{eDC} line has the same temperature dependence as J_∞^1 . J_e^0 values from creep (\bullet), 40 kHz (\square) and 30 MHz (\blacksquare) measurements; calculated J_e^0 temperature variation from equation (22)

the poly(styrenes), the high frequency region appears to be characteristic of a low molecular mass poly(propylene glycol); the value of the high frequency viscosity, $\eta_{DC} = 3.44 \times 10^7 \text{ Pa s}$ at -68°C , is close to the total viscosity of P1200 at the same effective temperature, $T - T_g$ (Table 2).

The remaining parameters, M , n and J_{eDC} , affect predominantly the shape of the calculated curves at low frequencies ($\omega < 1 \text{ rad s}^{-1}$). The width of the shoulder or plateau region of the G' curve increases with decreasing values of J_{eDC} . The major contribution to the measured quantity J_e^0 is from the first mode of the Rouse series. For the two component model, the measured value of J_e^0 is given by⁶:

$$J_e^0 = J_{eRouse} \left[\frac{\eta_{Rouse}}{\eta} \right]^2 + J_{eDC} \left[\frac{\eta_{DC}}{\eta} \right]^2 \quad (22)$$

For the chosen values of η_R , η_{DC} and J_{eDC} , J_{eR} must equal $2.0 \times 10^{-6} \text{ Pa}^{-1}$. Using equation (12), this value of J_{eR} corresponds to an effective molecular mass of 9500. This value of M is close to the value of \bar{M}_z shown in Table 2, and emphasizes the importance of higher moments of the molecular mass distribution in the determination of the steady state recoverable compliance.

The remaining parameter n , the number of effective Rouse modes, determines the magnitude of G' in the plateau region, Figure 6. The experimental curve for $G'(\omega)$ lies between the calculated curves for $n = 1$ and $n = 2$. On the assumption that the length of a Gaussian segment is equal to the separation between nodes for the highest order mode, a value $n = 2$ gives approximately 25 repeat units for the segment length: this is somewhat greater than values found for

other polymers. Adjustment of any or all of the other parameters of the combined model did not allow a reasonable fit with a greater number of modes.

Using the value of $M = 9500$ chosen to give the best fit, the temperature variation of the Rouse contribution to J_e^0 was calculated from equation (12), as shown in Figure 7. Values of the Davidson–Cole contribution to J_e^0 were estimated by fitting the combined model, equations (17) to (20), to the creep measurements at -68°C and the 40 kHz measurements conveniently reduced to 0°C . The error bars represent the maximum variation possible in J_{eDC} consistent with an acceptable fit between the measurements and the model behaviour. The line drawn through these two points, Figure 7, has almost the same temperature variation as J_∞ for P4000¹. This is consistent with the observations of the behaviour of many non-polymeric glass forming liquids¹³. The weighted sum of these two contributions, equation (22), gives the observed equilibrium recoverable compliance, J_e^0 . Values of J_e^0 , calculated in this way, agree well with those measured directly from creep recovery over the temperature range -50°C to -68°C . In this instance, where η_R and η_{DC} are similar in magnitude, the measured value of J_e^0 is much less than that calculated from equation (12). This effect has been reported previously for low molecular mass poly(styrenes)⁶. However, it should be noted that the combined model fails to account for the sudden decrease in J_e^0 observed at temperatures below -68°C . The values of J_e^0 at 5°C and 210°C , calculated from the combined model, also agree with the values of J_e^0 derived from 40 kHz and 30 MHz measurements. The derivation of these values was performed in the following manner.

The 30 MHz measurements of Barlow and Erginsav¹ were presented in the form of a complex-plane skewed-arc plot and fitted to the Davidson–Cole equation:

$$J_1(\omega)/J_\infty - J_2(\omega)/J_\infty = [J'(\omega)/J_\infty - 1] - j [J''(\omega)/J_\infty - 1/\omega\tau_m] = J_r/J_\infty (1 + \omega\tau_r)^\beta \quad (23)$$

As $\omega\tau_r \rightarrow 0$, $J_1(\omega) \rightarrow J_r$.

From the temperature variation of τ_r , the temperature for which $J_1(\omega)/J_r = 0.98$ was estimated, this temperature was assumed to be the effective temperature of the intercept J_r/J_∞ of the skewed arc with the real axis. The value of $J_e^0 (= J_r + J_\infty)$ may then be estimated from the extrapolated value of J_∞ at this temperature. The value of J_e^0 at 5°C was derived from the 40 kHz measurements in a similar manner. It is apparent from Figure 7 that J_e^0 does not have the same temperature dependence as J_∞ , the latter increasing linearly with temperature. However, over the limited range of temperatures used in these dynamic measurements, the variation of the ratio J_r/J_∞ is not sufficiently large to be apparent in the skewed arc plot. The decrease in the value of J_e^0 with increasing temperature has not been observed in the case of non-polymeric glass forming liquids. This reflects the predominance of the normal mode or entropic (Rouse) contribution to the elasticity in the low frequency region of the relaxation spectrum of polymer melts.

A direct comparison between the creep recovery and dynamic measurements is shown in Figure 8. For the purposes of this comparison, the dynamic measurements were transformed to the time domain using the approximation of Nimomiya and Ferry¹⁴:

$$J(t) \cong J'(\omega) + 0.40J''(0.40\omega) - 0.014J''(10\omega) \quad (24)$$

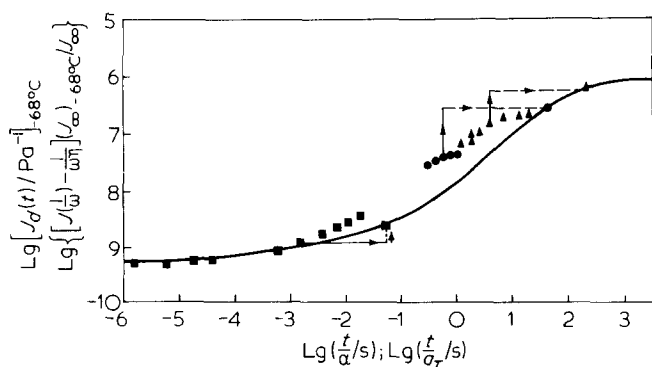


Figure 8 Creep recovery measurements taken from *Figure 2* (—) plotted as a function of time. Transformed dynamic data measured at 40 kHz (▲), 30 MHz (●) and 454 MHz (■) are normalized according to the temperature dependence of J_∞ and τ_m . Shown schematically are the shifts resulting from normalizing according to J_e^0 (—) and a_T (---) for the 40 kHz and 30 MHz data, and a_T (—) with an empirical compliance normalization (---) for the 454 MHz data

with $\omega \equiv 1/t$.

Before plotting, the values of $J(t)$ were normalized on the compliance scale according to the temperature variation of J_∞ and on the time scale according to the temperature variation $\alpha = (\tau_m)_T / (\tau_m)_{T_0}$, shown as the solid points in *Figure 8* with $T_0 = -68^\circ\text{C}$.

It is apparent from *Figure 8* that this normalization results in a fit which progressively deteriorates with increasing values of $J_d(t)$. It is also clear that no other compliance normalization alone can produce a satisfactory fit between the creep recovery and the dynamic measurements when the latter are normalized on the time scale according to α . An alternative time scale normalization factor is a_T derived from the creep recovery superposition, *Figure 3*. However, these measurements do not cover the required range of temperatures to allow normalization of all the dynamic measurements.

The mid-region of a viscoelastic dispersion corresponds to a range of frequencies close to $\omega\tau_m = 1$. The 40 kHz measurements were made in a region where $\omega\tau_m$ varies from 2.3×10^{-3} to 9.5×10^{-2} , whilst the corresponding region of measurement for the 30 MHz results extends from 5.3×10^{-2} to 1.7×10^{-1} . Thus, all these measurements lie in a frequency region near the terminal zone; that is, the low frequency side of the dispersion region. This would indicate that the appropriate compliance to be used as the compliance normalization factor is J_e^0 rather than J_∞ , the latter governing the high-frequency side of the dispersion.

However, the use of the temperature variation of J_e^0 for the compliance normalization factor requires a normalization factor along the time scale which is different from α . The effect of the two normalizations is shown schematically in *Figure 8*. The shifts along the time axis necessary for superposition of the dynamic data with the creep recovery curve are shown in *Figure 3* as a function of temperature.

Since the material responds as a linear viscoelastic liquid, frequency dependent and time dependent measurements are, in principle, directly comparable. Therefore, time scale normalization factors obtained from the creep measurements and from the dynamic measurements should be interchangeable. This implies that the shifts along the time axis obtained from the dynamic data form an extension to higher temperatures of the a_T values obtained from the creep recovery measurements. As shown in *Figure 3*, all the a_T values can be described by a single modified free volume equation, equation (7):

$$\ln(a_T) = -29.71 + 1028.9 (T/K - 171.2) \quad (25)$$

The 454 MHz dynamic measurements must, for consistency, also be normalized using values of a_T calculated using equation (25). The values of $\omega\tau_m$ for the 454 MHz data range from 10^6 at -60°C to 2.5 at $+40^\circ\text{C}$, thus covering a wide range of behaviour from the glassy region at low temperatures to near the centre of the dispersion region at high temperatures. It is therefore not possible to predetermine an appropriate compliance normalization factor. A value of the normalization factor for each point can be estimated by superposing the 454 MHz values with the creep recovery curve, after time scale normalization using a_T . This procedure is also shown schematically in *Figure 8*. The resulting compliance normalization factors are shown as a function of temperature in *Figure 9*.

Also shown in *Figure 9*, for comparison, are the temperature variations of J_∞ and J_e^0 , referred to a temperature of -68°C . The 30 MHz and 40 kHz compliance normalization factors, which were assumed to have the temperature dependence of J_e^0 , are shown in order to indicate the temperature range of these measurements. At temperatures below about -50°C the 454 MHz values follow the J_∞ variation, illustrating that, in the glassy region of response, the appropriate compliance normalization factor is given by J_∞ . At higher temperatures, the appropriate compliance normalization factor is intermediate between the values given by J_∞ and J_e^0 , tending towards the J_e^0 value at higher available limit of temperature.

In general, it may reasonably be assumed that in any viscoelastic liquid J_∞ and J_e^0 would have different temperature variations and thus care must be taken in selection of compliance normalization factors, which will be governed by

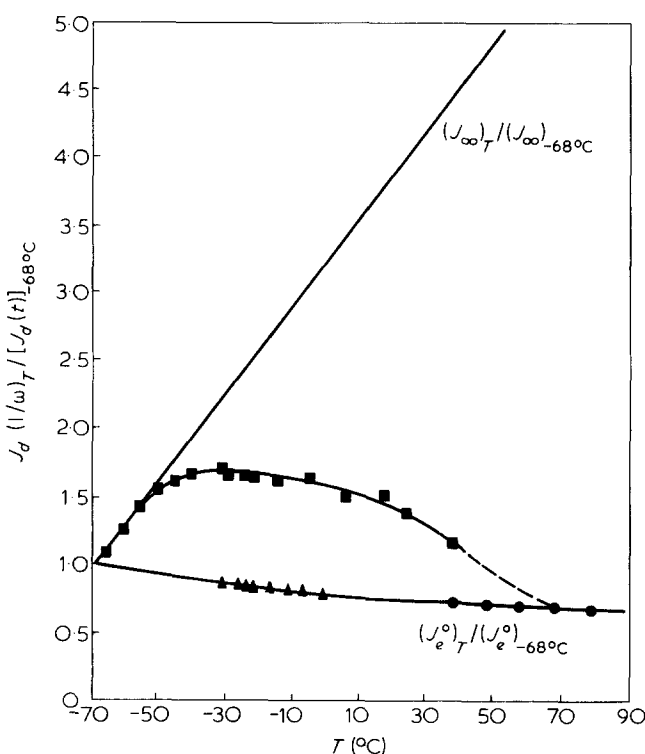


Figure 9 Temperature variation of compliance normalization factors for the 454 MHz measurements (■), compared with the temperature variation of J_∞ and J_e^0 . Also shown are the temperature ranges covered by the 30 MHz (●) and 40 kHz (▲) measurements

both the temperature and timescale of the measurements. The position of the measurement relative to the relaxation spectrum may be estimated from the value of $\omega\tau_m$. The compliance can then be normalized with respect to J_∞ when $\omega\tau_m \gg 1$ and to J_e^0 when $\omega\tau_m \ll 1$. For measurements made between these two extreme conditions, compliance normalization factors cannot be readily determined except by direct measurements.

In the light of this knowledge, the procedure adopted in the construction of the master creep recovery curve, *Figure 2*, may be re-examined. For measurements intermediate between the limiting short-time (glassy) and long-time (equilibrium) regions, the compliance normalization factors can only be obtained from additional isochronal measurements as a function of temperature. However, for the creep recovery measurements at temperatures above -68°C , which are close to the equilibrium steady-state region, the normalization factor should be close to the temperature variation of J_e^0 . As the variation is small, normalization can be neglected within the experimental error.

At temperatures below -68°C , the measurements extend from the equilibrium steady-state region towards the glassy region. The short-time region of these recovery curves should be normalized with respect to J_∞ . Over the limited temperature range of these measurements (-68 to -76°C) the variation of J_∞ is small, and again normalization can be neglected without introducing significant errors.

The remainder of these low-temperature measurements at longer times with values of $J_d(t) > 2 \times 10^{-8} \text{ Pa}^{-1}$, cannot be successfully normalized without the additional information mentioned above, and have therefore been omitted from the composite creep-recovery curve, *Figure 2*. However, the variation of J_e^0 with temperature between -68°C and -76°C can be estimated from the long-time limiting values of these curves. It appears therefore that the procedure adopted should not introduce significant errors and is the best practicable manner of reduction.

Taken together with earlier results for relatively low molecular mass poly(styrenes), the present results demonstrate that the observed behaviour can be ascribed to contributions from two processes. While the major contribution can be associated with the normal modes of the polymer molecule as a whole, a significant contribution is attributed to motions of smaller backbone units, akin to those previously observed in non-polymeric liquids. Moreover, since the latter are described in terms of a complex compliance, this must first be inverted to the modulus form before addition to the summation of the Rouse modes in order to calculate the effective overall modulus (equation (17)). However, this description is basically empirical and important parameters of the liquid, such as the compliance normalization factors, cannot be calculated *a priori*.

The slower (lower frequency) relaxation reported previously from dielectric studies by Baur and Stockmayer³ and by Alper *et al.*² can be related to the normal mode contribution reported here, while the faster and stronger dielectric process is related to the viscoelastically faster but weaker process. The small number of modes required to account for the low frequency viscoelastic behaviour is compatible with the narrowness of the dielectric spectrum for the slower process: no evidence for the existence of this relaxation process was found from either dielectric or viscoelastic measurements on the lower molecular weight P400 material.

The approximate single mode difference between the viscoelastic response of P400 and P4000 at 30 MHz, reported by Barlow and Erginsav¹ again agrees with the small number of

modes (1 or 2) found in the present work for the normal mode contribution to the behaviour of P4000. Qualitatively, if the above interpretation is correct, it may be argued that the small number of normal modes required to account for the observed behaviour is a consequence of the particular flexibility of the polymer backbone. This, in turn, implies weak restoring forces for displacements from equilibrium of the small backbone units, or, equivalently, comparatively low rotational barrier heights. This will produce relatively long time-constants for the local backbone motions with the consequence that the associated Davidson–Cole process will extend to lower frequencies (longer times) than would be the case with a more rigid backbone. Thus, for P4000 at -68°C , the longest retardation time in the Davidson–Cole spectrum is $\tau_r = 195$ s, whilst for one active mode only the corresponding normal mode relaxation time is $\tau_1 = 280$ s. Despite the fact that relaxation and retardation times are not directly comparable, there would nevertheless appear to be a considerable overlap in time between the Rouse and Davidson–Cole spectra. The Davidson–Cole process seems to provide a better description for the observed behaviour in this region than the higher order Rouse modes, which are apparently rendered inactive, the polymer mode contribution being accounted for by either the first or, at most, the first two Rouse modes. If the higher order modes exist in principle but do not contribute to the Rouse spectrum then the length of a Gaussian segment could be considerably smaller than the 25 repeat units, corresponding to the distance between nodes for the highest order mode ($n = 2$). This shorter length would be more in keeping with values found for other polymers.

ACKNOWLEDGEMENTS

This work has been supported by a Grant from the Science Research Council. Our former colleague, Dr R. W. Gray, is thanked for his contribution to the measurements reported here. We gratefully acknowledge the g.p.c. measurements made in the Department of Pure and Applied Chemistry, University of Strathclyde, through the good offices of Dr R. A. Pethrick.

REFERENCES

- 1 Barlow, A. J. and Erginsav, A. *Polymer* 1975, **16**, 110
- 2 Alper, T., Barlow, A. J. and Gray, R. W. *Polymer* 1976, **17**, 665
- 3 Baur, M. E. and Stockmayer, W. H. *J. Chem. Phys.* 1965, **43**, 4319
- 4 Barlow, A. J., Harrison, G., Richter, J., Seguin, H. and Lamb, J. *Lab. Pract.* 1961, **10**, 786
- 5 Plazek, D. J. *J. Polymer Sci. A-2*, 1968, **6**, 621
- 6 Gray, R. W., Harrison, G. and Lamb, J. *Proc. Roy. Soc. Lond. A* 1977, **356**, 77
- 7 Macconnachie, A., Vasudevan, P. and Allen, G. *Polymer* 1978, **19**, 33
- 8 Plazek, D. J. and O'Rourke, V. M. *J. Polymer Sci. A-2* 1971, **9**, 209–243
- 9 Ferry, J. D. 'Viscoelastic properties of polymers' Wiley, New York, 1970
- 10 Plazek, D. J. and Agarwal, P. *Proc. 7th Inter. Congress Rheol.* 1976, 488–489
- 11 Schwarzl, F. R. and Struik, L. C. E. *Adv. Mol. Relax. Proc.* 1967/68, **1**, 201
- 12 Yagii, K. and Maekawa, E. *Nippon Gamu Kyokaiishi* 1967, **40**, 46
- 13 Harrison, G. 'The dynamic properties of supercooled liquids', Academic Press, London 1976
- 14 Ninomiya, K. and Ferry, J. D. *J. Colloid Sci.* 1959, **14**, 36